

Robust Passivity-based Dynamical Systems for Compliant Motion Adaptation

Haohui Huang *Member, IEEE*, Yi Guo *Member, IEEE*, Genke Yang, Jian Chu, Xinwei Chen,
Zhibin Li, Chenguang Yang *Senior Member, IEEE*

Abstract—Motivated by human compliant behaviors during interacting with unknown environments and how motions and impedance to are adapted skillfully complete a task, this paper develops a motion planning scheme that is capable of generating a compliant trajectory online such that tracking desired contacting forces under a predefined motion task. First, an improved dynamical system (DS) is designed to generate an adaptive compliant scanning trajectory online from the original DS in terms of the contact forces and the desired scanning forces. Inspired by passivity analysis for the robot control system, a robust term is formulated to guarantee stability by considering the balance between environmental and robotic energy. Furthermore, we develop a state-constrained controller based on barrier Lyapunov function (BLF) to track the compliant DS motion and to ensure safety during scanning for the patient. Finally, comparative simulations are conducted to validate the general compliant capability of the proposed framework. We also instantiate our methodology through a use case of liver ultrasound scanning to demonstrate the stable and dynamic force tracking performance.

I. INTRODUCTION

With increasing implementations of robot occurred in various fields, the problems of control and motion planning have been rigorously studied over the past decades. As shown in Fig. 1, a form of compliant performance is indispensable for a myriad of robotic applications to ensure passivity and safety during interacting with environment [1], [2], [3]. Illustrating ultrasound robot as an example, a skilful scanning action generally requires a compliant pressing between patient's body surface and hand-held probe with appropriate contacting force [4], [5], [6]. Although humans are good at

*This work was supported in part by the China National R&D Key Research Program (2020YFB1711200), the Fellowship of the China Postdoctoral Science Foundation under Grant 2021M692068, and in part by the Open Fund Project of Fujian Provincial Key Laboratory of Information Processing and Intelligent Control (Minjiang University) (No.MJUKF-IPIC202103).

Haohui Huang is with Department of Automation, Shanghai Jiao Tong University, Shanghai 200240, China, with Ningbo Artificial Intelligence Institute of Shanghai Jiao Tong University, Ningbo, Zhejiang 315000, China, and also with Fujian Provincial Key Laboratory of Information Processing and Intelligent Control, Minjiang University, Minjiang 353099, China.

Yi Guo, Genke Yang and Jian Chu are with Department of Automation, Shanghai Jiao Tong University, Shanghai 200240, China, and also with Ningbo Artificial Intelligence Institute of Shanghai Jiao Tong University, Ningbo, Zhejiang 315000, China.

Xinwei Chen is with Fujian Provincial Key Laboratory of Information Processing and Intelligent Control, Minjiang University, Minjiang 350108, China.

Zhibin Li is with Department of Computer Science, University College of London, 66-72 Gower Street, WC1E 6BT, UK

Chenguang Yang is with Bristol Robotics Laboratory, University of the West of England, Bristol, BS16 1QY, UK.

Corresponding authors are Chenguang Yang cyang@ieee.org and Genke Yang gkyang@sjtu.edu.cn

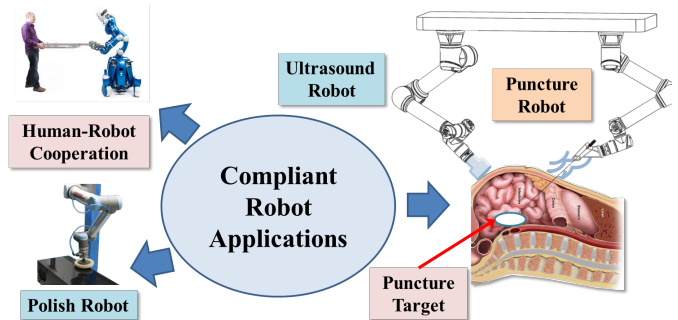


Fig. 1. Applications of robot-environment compliant interaction.

adapting in dynamic environment (with potential uncertainties and disturbance), robots dominate in efficiency, stable and precision force/position control during performing repetitive actions which contributes to further standardize ultrasound scanning. Thus, ultrasound-guide puncture robot has received widespread attention, which is able to release the scanning burden from physician and focus their more attention on disease judgement [7], [8], [9].

Recently, admittance/impedance control [10], virtual-spring haptic feedback control [11], force/position switching control [12] have been extensively adopted in ultrasound scanning robot system. In technical note, a desired compliant performance based on such methods requires perfect knowledge about muscle surface and robotic model which are notoriously difficult to obtain. In this regard, numerous challenges between body modelling, motion planning and compliant control must be addressed.

For the purpose of accomplishing tasks by robot, it is essential to seek a flexible scheme that is able to efficiently and quickly transfer new skills to robot [13], [14], [15]. Robotic motion planning with stable DS has become the forefront of present study to deal with task trajectory encoding problems [16], [17]. Notwithstanding past researches have demonstrated excellent motion planning ability of DS, compliant performance and robustness are also required to resist the force perturbation from interaction. Optimal feedback control [18] has been used to reconstruct a force adaptation DS under force field with minimizing the value of cost function. By linearizing the dynamics model of robot, a global optimal solution can be obtained in linear-quadratic-Gaussian (LQR) method. In [19], a motor learning model is developed to preserve the dynamical and kinematical features reaching motion under an unknown force field. Recently, an adaptive parameterized DS framework has been proposed to accommodate the influenced by human-

robot interaction by means of impedance controller [20]. In the following, they designed a novel DS framework to generate an adaptive motion and contact forces [21], addressing the challenges of robustness of real-world uncertainties and providing new insights into compliant robot-environmental interaction.

While the above researches mainly concentrate on the adaptation and compliance of DS, stability and safety for robot-environment interaction is equally critical for real robotic system. In this regard, classical robotic control literatures have extensively discussed the problems about state constraints in case of physical stoppages or upper limit of running speed [22], [23], [24]. Recently, a novel motion constraints learning framework is proposed in terms of zeroing barrier functions (ZBFs) from human demonstrations, which provides a promising insight into space constraints from motion planning perspective [25]. As shown in the past works, it is popular for researchers to study a robust or coupling terms to accommodate the motion during interacting with environment.

Different from these approaches, we hope to make a forward step to cope with the problems of compliant interaction through monitoring the energy balance between environment and DS at scanning motion planning level instead of robotic control perspective. The contributions and novelties of this article with respect to the state-of-the-art are summarized as follows:

- 1) A novel adaptive DS is designed to deal with compliant motion generation under robot-environment interaction, which is capable to achieve force tracking without a priori knowledge about environmental impedance model [26]. Notably, our approach only adopts the error information between contacting force and desired tracking force to adjust the desired trajectory from motion planning level instead of motion control level, which offers a different insight to the problems of compliant interaction.
- 2) In order to maintain energy conservation between the DS and the environment, a passivity observer is deduced so as to accommodate the unknown dynamical environment with respect to robustness and adaptability of DS.
- 3) From robotic control point of view, a tan-barrier Lyapunov function is utilized to achieve the predefined performance such that a safety constraint control can be guaranteed.

The remainder of this paper is organized as follows. In Section II, we introduce the fundamental problems and important theory about the proposed method. Next, the principle of our proposed methodology is introduced and stability of designed system is given in Section III. Section IV provides the convincing simulation and experiment results to validate the proposed method. Finally, a conclusion is drawn in Section V.

II. PROBLEM FUNDAMENTALS

In this section, all the base methods utilized in this article are presented consisting of dynamic model of robot, state-constraints controller we use subsequently and the principle of DS. The novel contributions of our proposed method will be illustrated in Section III.

A. Robot Dynamic Model in Task Space

In the literature, the case of robot-environment interaction in Cartesian space is executed through a multi-link manipulator. In order to cope with the compliant control problems related to robot environment interaction, an ideal impedance model can be concerned with a mass-damping-spring system [27]

$$\mathbf{D}_c(q)\ddot{\tilde{\theta}} + \mathbf{C}_c(q, \dot{q})\dot{\tilde{\theta}} = F_e - \mathbf{M}_I\dot{\tilde{\theta}} - \mathbf{K}_I\tilde{\theta} \quad (1)$$

where $\tilde{\theta} \in \mathbb{R}^m$ denotes the tracking error in m -dimension Cartesian space with $\tilde{\theta} = \xi - \xi_d$. ξ and ξ_d represent the actual and desired position of the end-effector, respectively. F_e is the environmental contacting force. $\mathbf{D}_c(q) \in \mathbb{R}^{m \times m}$ and $\mathbf{C}_c(q, \dot{q}) \in \mathbb{R}^{m \times m}$ denote the positive-definite inertial matrix and Coriolis centrifugal forces vector. $\mathbf{M}_I \in \mathbb{R}^{m \times m}$ and $\mathbf{K}_I \in \mathbb{R}^{m \times m}$ are the ideal damping and stiffness matrices. $q \in \mathbb{R}^k$ denotes joint position of the k -link manipulator which can be derived from the well-known inverse kinematic model and nonsingular Jacobin matrix $J(q) \in \mathbb{R}^{k \times m}$ as follow

$$\dot{q} = J^{-1}(q)\dot{\xi} \quad (2)$$

B. State-Constraints Motion Control

With the purpose of clarity, the principle of state-constraints motion control is introduced in this part. To be specific, the controller we use is defined as [28]

$$F_c = - \begin{bmatrix} \frac{e_{11}}{\cos^2(\frac{\pi e_{11}^2}{2\gamma_1^2})} \\ \vdots \\ \frac{e_{1n}}{\cos^2(\frac{\pi e_{1n}^2}{2\gamma_n^2})} \end{bmatrix} + \hat{\mathbf{D}}_c \dot{\alpha}_1 + \hat{\mathbf{C}}_c \alpha_1 + \hat{\mathbf{G}}_c - \delta_p e_2 - \delta_r \operatorname{sgn}(e_2) + F_e \quad (3)$$

where $\delta_p = \operatorname{diag}\{\delta_{p1}, \dots, \delta_{pn}\}$ and $\delta_r = \operatorname{diag}\{\delta_{r1}, \dots, \delta_{rm}\}$ are tuned parameters with $\delta_{pi} > 0$ and $\delta_{ri} > 0$. $e_1 = \xi - \xi_d$ and $e_2 = \dot{\xi} - \dot{\alpha}_1$ denote the Cartesian tracking error variable with virtual control signal designing as

$$\alpha_1 = \dot{\xi} - \Delta_1 Y \quad (4)$$

where $\Delta_1 = \operatorname{diag}\{\delta_{11}, \dots, \delta_{1n}\}$ represents a constant positive matrix with $\delta_{1n} > 0$. According to L'Hospital's rule, we design variable $Y = [y_1, y_2, \dots, y_n]^T$ as a nonsingularity matrix with $y_n = (\gamma_n^2 / 2\pi e_{1n}) \sin(\pi e_{1n}^2 / \gamma_n^2)$ where γ_n determines the constraint of system states by $\|e_{1n}\| < \gamma_n$. $\hat{\mathbf{D}}_c$, $\hat{\mathbf{C}}_c$ and $\hat{\mathbf{G}}_c$ are approximated through Broad Fuzzy Neural Network (BFNN)

$$\begin{aligned} \hat{\mathbf{D}}_c &= \hat{W}_D^T h_D + \varepsilon_D \\ \hat{\mathbf{C}}_c &= \hat{W}_C^T h_C + \varepsilon_C \\ \hat{\mathbf{G}}_c &= \hat{W}_G^T h_G + \varepsilon_G \end{aligned} \quad (5)$$

where h_D , h_C and h_G are transfer membership functions integrated with the information of neurons and fuzzy rules. ε_D , ε_C and ε_G denote the approximation errors. \hat{W}_D , \hat{W}_C and \hat{W}_G represent the adaptive neural weight whose updated laws are designed as:

$$\begin{aligned} \dot{\hat{W}}_D &= -v_D \alpha_1 e_2 - \beta_D \hat{W}_D \\ \dot{\hat{W}}_C &= -v_C \alpha_1 e_2 - \beta_C \hat{W}_C \\ \dot{\hat{W}}_G &= -v_G e_2 - \beta_G \hat{W}_G \end{aligned} \quad (6)$$

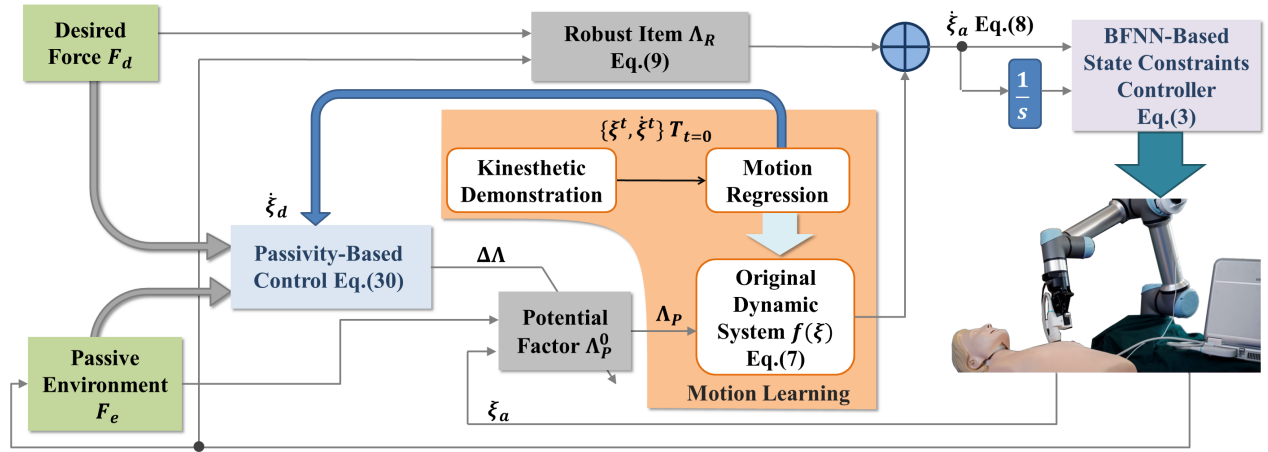


Fig. 2. Adaptive compliant motion control architecture of the proposed method which consists of motion learning and state constraints controller.

where β_D, β_C and β_G are the predefined parameters to guarantee the robustness of BFNN. v_D, v_C and v_G denote the update gain of neural work. In this way, the detail principle of transfer membership functions and the proof of stability of state constraint controller can be refer to [28].

C. Motion Planning with Dynamical Systems

DS is one of the most versatile and flexible methods in the field of robot motion planning researches which is suitable for real-time adaptive motion planning and robot-environment interaction scenes. To be specific, differential equations are adopted to model the motion characteristics such that the next motion only depends on the current state of system, which can provide a compromise performance between the motor generation and the computational burden.

In this part, we introduce a short outline and the most essential theory of DS as needed in our work. Generally, an original autonomous DS formulation is formulated as

$$\dot{\xi}_d = f(\xi) \quad (7)$$

where ξ_d denotes the desired discrete motion state of the system, e.g. the task's position in Cartesian space. $f(\cdot): \mathbb{R}^m \rightarrow \mathbb{R}^m$ is a continuous function which is used to approximate a specific motion model such as stepping movement, reaching out for an object. One prerequisite of dealing with motion planning and perturbation problems through DS is the stability theory [29]:

Theorem 1: The DS function $f(\xi)$ is globally asymptotically stable if $\lim_{t \rightarrow \infty} f(\xi^t) = f(\xi^*) = 0$, where ξ^* denotes the target state of DS.

Previous research has proven that globally asymptotically stable is essential for trajectory adaptation instantly in the process of robot-environment interaction [29]. In our study, the following assumptions are worth noticing throughout the motion planning such that an adaptive and stable trajectory can be obtained.

Assumption 1: The non-linear continuously DS is globally asymptotically stable which is able to derive the motion

starting from any points and ending at the single attractor point.

Assumption 2: The unknown interacting object is assumed to be continuous and smooth.

III. PASSIVITY BASED DS ADAPTATION AND CONTROL

In this section, a novel DS framework via passivity based control is proposed to endow robots with such ability through motion adaptation. In addition, a Broad Fuzzy Neural Network (BFNN) state constraints controller is designed to guarantee a safety interaction between robot and environment. Fig. 2 illustrates the architecture of the proposed system that incorporates these points.

A. Adaptive Dynamical Systems Design under Interaction

As shown in Fig. 2, an original desired task motion ξ_d is first obtained from some conventional demonstration methods which eventually models as a DS $f(\xi)$. Aiming at accommodating the desired motion during interacting with the environment, the desired motion ξ_a is reshaped through the proposed framework while preserving the robustness and adaptability of DS which is defined as

$$\dot{\xi}_a = \Lambda_P f(\xi) + \Lambda_R \quad (8)$$

where Λ_P and Λ_R denote the adaptive potential factor and robust item respectively. In this framework, the adaptive potential factor Λ_P is developed in terms of passivity observer (PO) whose theoretical foundation will be discussed hereinafter. In [30], the parameters of modulation item Ξ_f are obtained through trial and error which limits the fidelity of the motion planner. To proceed, this paper brings forward a solution by simplifying the modulation to a robust item which is designed as

$$\Lambda_R = K_r \cdot e_f \quad (9)$$

where $e_f = F_e - F_d \in \mathbb{R}^m$ denotes the force tracking error during interaction. K_r is the scaling factors to modulate the effect from force error. It is worth noting that the desired contacting

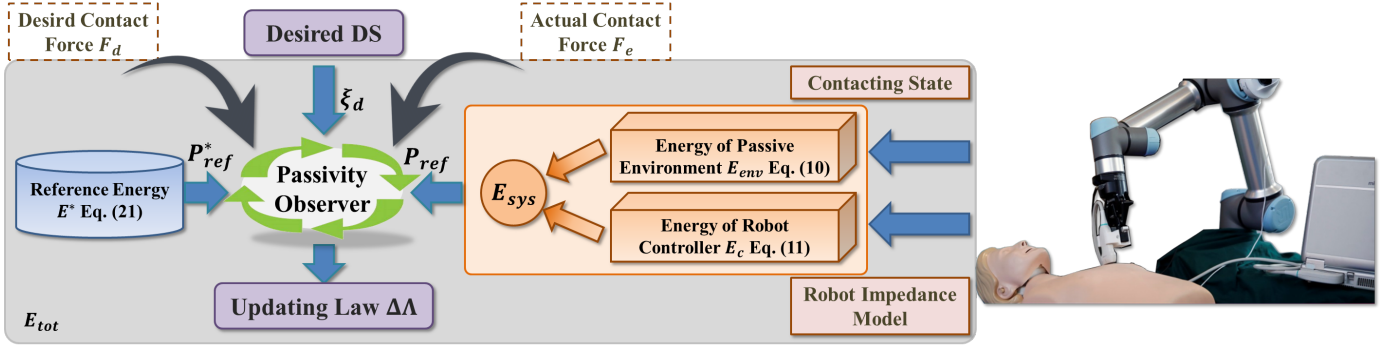


Fig. 3. Depicted overall framework including Desired DS, passivity observer, reference energy provider and robot motion controller interacting with a passive environment.

force F_d which is obtained from the task demonstration will be zero commonly while the end-effector is moving in the free space.

B. Passivity Analysis for the Adaptive Dynamical Systems

As we analysed before, one prerequisite of safely compliant DS is stability in contact with environment. In this part, passivity-based control is utilized to remain stability of the overall DS and the corresponding analysis is solidly grounding through the PO. Fig. 3 shows a schematic explanation of the proposed framework.

Commonly, most DS can be regarded as a system with state space model

$$\begin{aligned} \dot{x} &= \mathcal{A}(x, u) \\ y &= \mathcal{B}(x, u) \end{aligned} \quad (10)$$

where $x \in \mathbb{R}^k$ denotes the state of system. $u, y \in \mathbb{R}^l$ represent the input and output of Eq. (10). Afterwards, we call it passive if input $u : [0, \sigma] \rightarrow \mathbb{R}^l$ and output signal y satisfy the follow inequality with $\sigma > 0$ and the initial state $x_0 \in \mathbb{R}^m$ [31]

$$E(x(\sigma)) - E(x_0) \leq \int_0^\sigma u^T(t)y(t)dt \quad (11)$$

where $E(\cdot) : \mathbb{R}^k \rightarrow \mathbb{R}_+$ denotes an energy storage function. In other words, a system is passive in derivative form of Eq. (11) that

$$\dot{E} \leq u^T y \quad (12)$$

From the adaptive dynamical system Eq. (8) with pair $\langle \xi_a, -F_e \rangle$ point of view, one storage function which scales the energy of passive environment can be defined as

$$\dot{E}_{env} \leq -\xi_a^T F_e \quad (13)$$

Next, we establish another energy storage function to scale the control energy with the consideration of Cartesian impedance closed loop dynamic Eq. (1) as

$$E_c = \frac{1}{2} \dot{\theta}^T \mathbf{D}_c \dot{\theta} + \frac{1}{2} \dot{\theta}^T \mathbf{K}_I \dot{\theta} \quad (14)$$

Upon taking the derivative of storage function with closed loop dynamic Eq. (1), we can get

$$\begin{aligned} \dot{E}_c &= \dot{\theta}^T \mathbf{K}_I \dot{\theta} + \frac{1}{2} \dot{\theta}^T \mathbf{D}_c \ddot{\theta} + \dot{\theta}^T \mathbf{D}_c \ddot{\theta} \\ &= \dot{\theta}^T \mathbf{K}_I \dot{\theta} + \frac{1}{2} \dot{\theta}^T \mathbf{D}_c \ddot{\theta} \\ &\quad + \dot{\theta}^T (-\mathbf{C}_c \dot{\theta} - \mathbf{M}_I \ddot{\theta} - \mathbf{K}_I \dot{\theta} + F_e) \\ &= \dot{\theta}^T F_e + \underbrace{\frac{1}{2} \dot{\theta}^T (\mathbf{D}_c - 2\mathbf{C}_c) \ddot{\theta}}_{=0} - \underbrace{\dot{\theta}^T \mathbf{M}_I \ddot{\theta}}_{\geq 0} \\ &\leq \xi^T F_e - \xi_a^T F_e \end{aligned} \quad (15)$$

To proceed, the energy storage function of the whole passive interaction system containing robot and environment can be defined as

$$E_{sys} = E_c + E_{env} \quad (16)$$

Submitting the environment Eq. (13) and impedance close loop dynamic storage Eq. (15) function into Eq. (16) and taking the time derivation, we have

$$\begin{aligned} \dot{E}_{sys} &= \dot{E}_c + \dot{E}_{env} \\ &\leq \xi^T F_e - \xi^T F_e - \xi_a^T F_e \\ &= -\xi_a^T F_e \end{aligned} \quad (17)$$

Considering the desired motion ξ_a which is generated from the adaptive DS and desired tracking force F_d from task demonstration, we define a reference energy as

$$P_{ref} = -\xi_a^T F_e \quad (18)$$

According to adaptive DS Eq. (8), the whole passive interaction system storage function can be rewritten as

$$\begin{aligned} \dot{E}_{sys} &\leq -\xi_a^T F_e \\ &= -(\Lambda_R + \Lambda_P \xi_d)^T F_e \\ &= -(\Lambda_P \xi_d)^T F_e - \Lambda_R^T F_e \end{aligned} \quad (19)$$

Specially, the latter item of Eq. (19) is equivalent as

$$\begin{aligned} -\Lambda_R^T F_e &= -(F_e - F_d)^T K_r F_e \\ &= \underbrace{-(F_e - F_d)^T K_r (F_e - F_d)}_{\leq 0} - (F_e - F_d)^T K_r F_d \\ &\leq -\Lambda_R^T F_d \end{aligned} \quad (20)$$

In this case, we can further obtain from Eq. (19) and Eq. (20) that

$$\dot{E}_{sys} \leq -(\Lambda_P \dot{\xi}_d)^T F_e - \Lambda_R^T F_d \quad (21)$$

At the same time, the reference energy, taking the passivity analysis of the interaction system between adaptive DS and environment into account, can be redefined as

$$P_{ref} = -(\Lambda_P \dot{\xi}_d)^T F_e - \Lambda_R^T F_d \quad (22)$$

C. Potential Factor Adaptation Based on Passivity Observer

In this part, the design of passivity observer is elaborated in terms of the analysis of passive dynamical system. As discussed before, the compliant motion is generated from the adaptive DS according to the environmental contacting force F_e and demonstrated desired force F_d . Ideally, the proposed scheme is committed to produce a trajectory which is able to track the desired force F_d , i.e. $F_e = F_d$. At this moment, the robust item Eq. (9) becomes zero and the ideal reference energy is then given by:

$$P_{ref}^* = -(\Lambda_P \dot{\xi}_d)^T F_d \quad (23)$$

The ideal reference storage function of passive interaction system can be derived the ideal reference energy as

$$\dot{E}^* \leq -P_{ref}^* \quad (24)$$

Thereby, we give the storage function of the overall system which consists of passive interaction system Eq. (17) and reference system Eq. (24) as

$$E_{tot} = E_{sys} + E^* \quad (25)$$

whose time derivation is calculated as

$$\dot{E}_{tot} \leq P_{ref} - P_{ref}^* \quad (26)$$

According to the passive control theory, the passivity of the overall system can be guaranteed if $\dot{E}_{tot} \leq 0$. In this regard, the passivity observer can be established as

$$\begin{cases} \text{Non-passive} & P_{tot} > 0 \\ \text{Passive} & P_{tot} \leq 0 \end{cases} \quad (27)$$

where

$$\begin{aligned} P_{tot} &= P_{ref} - P_{ref}^* \\ &= -(\Lambda_P \dot{\xi}_d)^T F_e - \Lambda_R^T F_d + (\Lambda_P \dot{\xi}_d)^T F_d \end{aligned} \quad (28)$$

Although the previous work [30] has capability to generate a compliant interaction trajectory at the motion planning level, such scheme is insufficient for tackling the problem of dynamical force contacting task. For this reason, the adaptation is adopted to the compliant motion planning, as well as remaining the stability of system during dynamical force interaction under the criterion of passivity observer. To be specific, the adaptive potential factor in Eq. (8) is updated through iterative learning in every time sample by

$$\Lambda_P = \Xi_P + K_u \Delta \Lambda \quad (29)$$

where K_u is a positive learning rate. $\Delta \Lambda$ represents the updating law which is determined by passivity observer as

$$\begin{aligned} \Delta \Lambda &= P_{tot}^\dagger \\ &= -(\Lambda_P \dot{\xi}_d) F_e^T - \Lambda_R F_d^T + (\Lambda_P \dot{\xi}_d) F_d^T \end{aligned} \quad (30)$$

Ξ_P denotes the initial potential factor which was designed in our previous work [30], scaling the effect of contacting between end-effect and environment in terms of force feedback, and it can be written as

$$\Xi_P = \begin{cases} Q(\omega)H(\rho)Q(\omega)^{-1} & F_e > 0 \\ \mathbf{I} & F_e = 0 \end{cases} \quad (31)$$

where $\omega = [\omega_1, \omega_2, \dots, \omega_m] = \frac{F_e}{\|F_e\|}$ denotes the unit normal

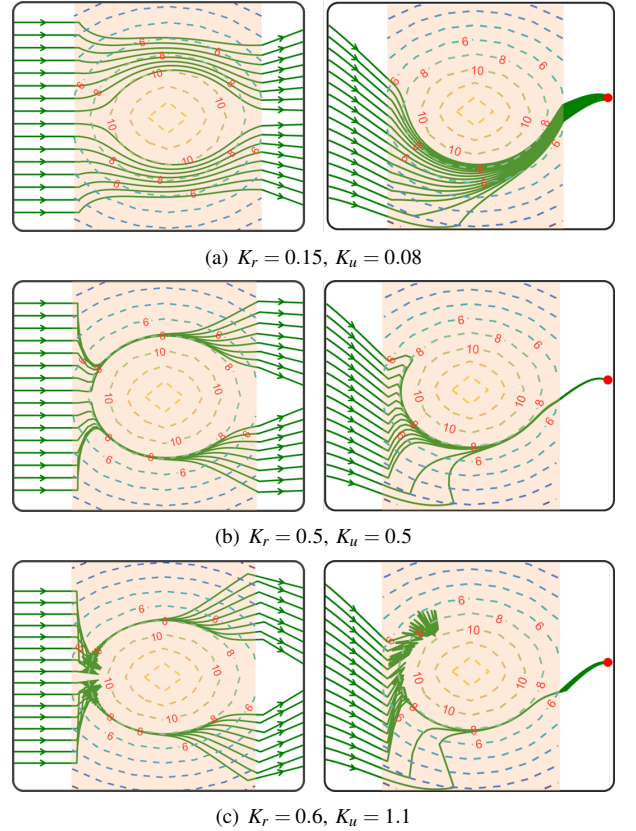


Fig. 4. Comparison results of compliant motion planning under different choices of proportion factor K_r and learning rate K_u .

vector. The basic matrix $Q(\omega) \in \mathbb{R}^{m \times m}$ can be derived by

$$Q(v) = [\mathbf{W}^1 \ \dots \ \mathbf{W}^D] = \begin{bmatrix} \omega_1 & -\omega_2 & \dots & -\omega_m \\ \omega_2 & \omega_1 & 0 & \dots \\ \vdots & 0 & \ddots & \vdots \\ \omega_m & 0 & \dots & \omega_1 \end{bmatrix} \quad (32)$$

In addition, $\rho = \sum_{i=1}^m (F_d(i)/F_e(i))$ in Eq. (31) is the force operator which determines the eigenvalues matrix given by

$$H(\rho) = \text{diag}\{\lambda_1, \lambda_2, \dots, \lambda_m\} \quad (33)$$

where $\lambda_1 = 1 - \frac{1}{|\rho(F_e)|}$ and $\lambda_i = 1 + \frac{1}{|\rho(F_e)|}$, for $2 \leq i \leq m$. F_d is the desired task contacting force while interaction.

Remark 1: Compared with the conventional impedance control, the superiority of designed DS-based passivity observer is that the environmental impedance model is no longer required for compliant interaction. Note that in this paper, only K_r and K_u need to be chosen to balance the compliant and stability performance of the proposed method.

IV. SIMULATION RESULTS

In this part, the proposed scheme is validated through numerical simulations, aiming at demonstrating the capability of compliant and flexible motion generation in unknown environment. In our simulations, contact force feedback is considered to modulate the desired task motion during the interaction. To be simplified, we assume that the robot is able to track the DS motion perfectly which means there is no need to consider the design and performance of controller.

A. Case 1: Performance of Stability in Unknown Force Field

In order to demonstrate the stability and effect of choosing different parameters of the proposed methods, simulations of DS planning with different start and target points are conducted under an unknown force field. Firstly, we assumed that the DS is asymptotically stable throughout all the simulations. For simplicity but without loss of generality, two models of DS using in this case are defined as

$$DS_1 \begin{cases} \dot{\xi}(1)_d = -\xi(1) \\ \dot{\xi}(2)_d = -\xi(2) \end{cases} \quad (34)$$

$$DS_2 \begin{cases} \dot{\xi}(1)_d = -\xi(1) \\ \dot{\xi}(2)_d = -\xi(1) \cos(\xi(1)) - \xi(2) \end{cases} \quad (35)$$

The comparison simulation results of all these DS are shown in Fig. 4. In this scenario, different DS have passed through a disturbed force field as shown in the yellow region along with the corresponding force equipotential lines which is modelling as

$$\begin{aligned} F_e(1) &= -F_0 \exp(\xi(1)^2 + \xi(2)^2) \\ F_e(2) &= \sqrt{F_0^2 - F_e(1)^2} \end{aligned} \quad (36)$$

where $F_c = K_e(R_0 \sqrt{\xi(1)^2 + \xi(2)^2})$ with $K_e = 8$ and $R_0 = 2$ in this simulation respectively. Additionally, we set the desired contacting force as $F_d = 8$ in the process of movement in the force field. From these results, we can see that the compliant adaptive motions generated by the proposed method remain stable with different set of parameters. Nevertheless, too small values may lead to poor capability of force tracking under disturbance, i.e. large force tracking error, and vice versa. It is obvious that too large parameters may also result in motion jitter or even system instability.

B. Case 2: Capability of Motion Generalization in case of Dynamical Force Tracking

In this part, we validate our approach to demonstrate the capability of dynamical force tracking and stability of the overall passive DS. To proceed, an adaptive motion is first

generated through the proposed passive DS which is defined as

$$\dot{\xi}_d = \begin{bmatrix} r_a \cos(\theta_a) + r_0(1) \\ r_a \sin(\theta_a) + r_0(2) \end{bmatrix} \quad (37)$$

where r_a and θ_a denote the radius and angle with respect to the center of contacting object in polar coordinates whose velocity are set as

$$\begin{aligned} \frac{\partial r_a}{\partial t} &= -K_a(r_a - r_0) \\ \frac{\partial \theta_a}{\partial t} &= 0.5 \end{aligned} \quad (38)$$

where $K_a = 4$ and $r_0 = 0.25$. Meanwhile, the model of contacting object is designed as an irregular shape force field whose boundary is defined as

$$\eta_o = \begin{bmatrix} \varepsilon_1 \cos(v) \\ \varepsilon_2 \text{sgn}(v)(1 - \cos(v))^{2\mu_1} \frac{1}{2\mu_2} \end{bmatrix} \quad (39)$$

where ε_1 , ε_2 , μ_1 and μ_2 are the predefined parameters to determine the shape of object. v denotes the angle of boundary, i.e. $v = \arctan(\xi(2)/\xi(1))$. During contacting with the irregular object, we assume that the contacting force is inversely proportional to the distance to the center of the object, e.g. $F_e = d_r(r_0 - r_a)/r_0$.

Fig. 5 shows the related simulation results of adaptive motion planning in case of dynamic force tracking through the proposed method. Firstly, we set the desired force, changing from 5N to 17N for every ten second and the DS parameters are set as $K_r = 0.2$ and $K_u = 0.02$ respectively during the whole motion. As shown in Fig. 5(a), it can be easily concluded that the adaptive motion stays stable during contacting the object at all time by the proposed method even the desired force is changed in time. The curves illustrated in Fig. 5(b)-(e) have shown the performance of dynamic force tracking, in which the ordinate is the scale of contacting force while the abscissa is the time of motion. From these figures, the adaptive motion is able to track with the desired force. Although the error of force tracking is mutation suddenly at the moment of desired force changing, it returns to steady immediately and remains within 1N. Compared with previous work [27], another significant progress is that the proposed method can also valid for the attractor point of adaptive DS whose location is in the region of object as shown in Fig. 5(a), which relaxes the strict assumption in [30] such that expanding the application in robot-environment interaction. Furthermore, the total energy of passive DS is investigated in Fig. 5(f) which indicates that the passive energy remains stable during the interaction even the change of desired force.

V. EXPERIMENTAL RESULTS

A qualified ultrasound scanning action is required to fully consider the physical characteristics of patient including body shape, skin smoothness and scanning position. It is scarcely possible to establish a standard schedule for robot system to complete the scanning for different people. Aiming at further demonstrating the adaptive and compliant capability

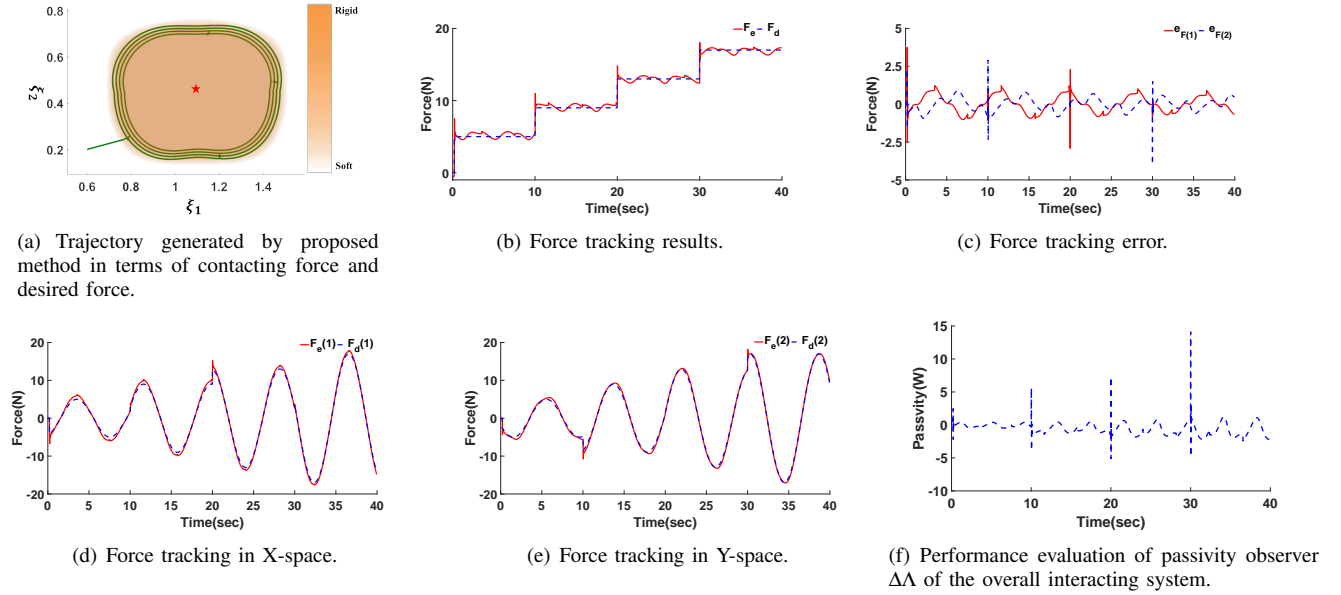


Fig. 5. Simulation Results of compliant force tracking in phase of motion planning.

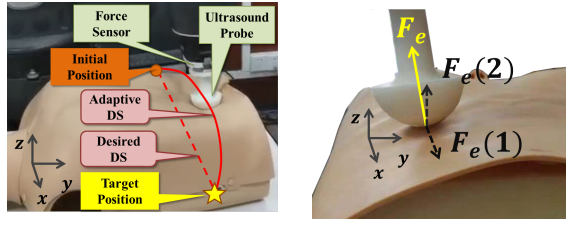


Fig. 6. Experimental platform for robot ultrasound scanning.

TABLE I
VALUES AND MEANINGS OF PARAMETERS IN CONSTRAINT CONTROL AND PASSIVITY LEARNING

Parameter	Description	Value
$[\gamma_1, \gamma_2, \gamma_3]$	Constraints parameters of system state	$[0.05, 0.05, 0.05]$
Δ_1	Virtual control gain	$\text{diag}\{23, 23, 25\}$
δ_p	Constraint motion control gain	$\text{diag}\{3, 3, 3\}$
δ_r	Constraint motion control gain	$\text{diag}\{50, 50, 75\}$
β_D	Robust item of BFNN	5
β_C	Robust item of BFNN	5
β_G	Robust item of BFNN	5
v_D	Update gain of NN	0.3
v_C	Update gain of NN	0.3
v_G	Update gain of NN	0.3
K_r	Scaling factor of force error	0.1
K_u	Passivity learning rate	$\text{diag}\{0.5, 0.5\}$

of the proposed method, experiments imitating liver ultrasound scanning on robotic system autonomously is conducted.

Fig. 6(a) shows the experimental platform. Ultrasound scanning is executed by a 7 degree-of-freedom (DOF) Baxter collaborative robot, equipped with a Mini45 Force/Transducer Sensor to measure the contacting force and scanning probe made by 3D printer at the end-effector of manipulator. In the experiment, the controller is developed under Robot Operating System (ROS), whose Software Development Kit (SDK) is

provided from Rethink Company and the control rate is set as 100 Hz.

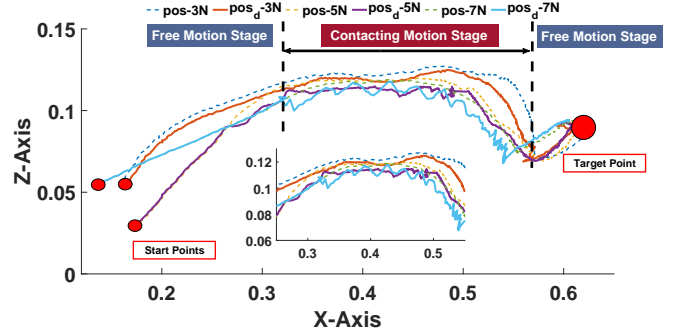


Fig. 7. Trajectory tracing under different desired contacting force.

In order to evaluate the performance of the proposed method in the presence of uncertainty, there is no priori knowledge of the patient model during the whole experiment. Furthermore, As shown in Fig 6(a), we first design an initial desired DS, scripting a simple straight way to converge to the target point from any initial position

$$\dot{\xi}_d = -\mathbb{Q}(\xi - \xi_g) \quad (40)$$

where $\mathbb{Q} = \text{diag}\{3, 3, 3\}$ in this experiment. Target point is set as $\xi_g = [0.75, 0.16, 0.05]$. While the probe is scanning on the surface of body, the desired DS ξ_d will be modulated adaptively through Eq. (8) to ξ_a so as to achieve the compliant interaction.

In this experiment, we design different force tracking scenarios for the robot to scan along the skin of patient, e.g. $F_d = 3N, 5N$ and $7N$ to verify the capability of compliant motion generation of the proposed method. To simplify the question but without loss of generality, the desired motion is only modulated in x and z axis in this case. Thus, the tracking force F_d and F_e represents the force of the normal vector of

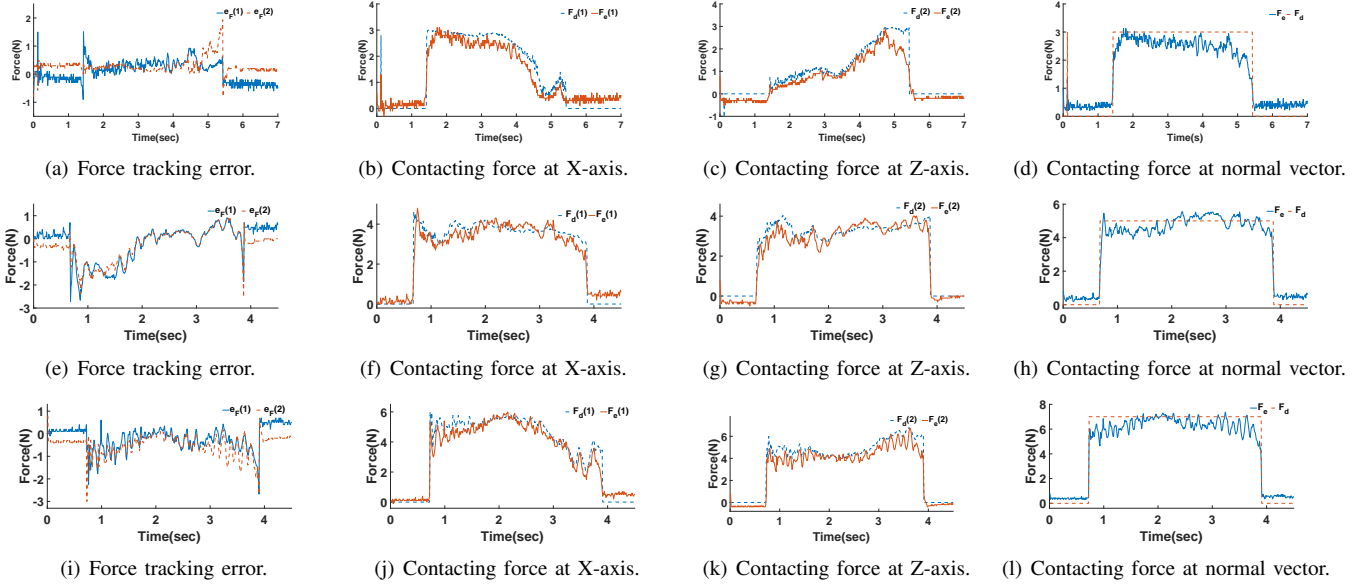


Fig. 9. Experimental results of force tracking under different desired contacting force. (a)-(d) are the force tracking results under 3N desired contacting force. (e)-(h) are the force tracking results under 5N desired contacting force. (i)-(l) are the force tracking results under 7N desired contacting force.

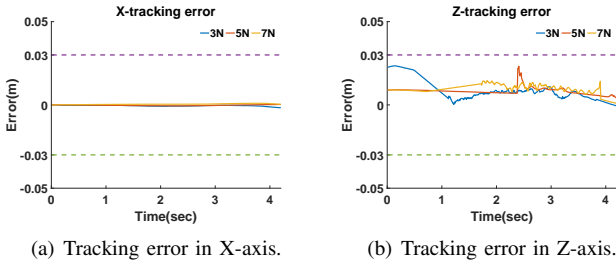


Fig. 8. Simulation results of tracking error by using the position state constraint controller.

the contacting surface and then it will be decomposed into horizontal and vertical vector as shown in Fig 6(b).

As for the state constraint controller using in this experiment, the value of parameters are listed in Table. I. Fig. 7 shows the scanning motion tracking results by using the proposed methods under a two-dimension space, e.g. X , Z axis, where we can see that the proposed method successfully modified the original DS to adapt the external unknown contacting force so as to achieve a compliant interacting behavior.

In this experiment, a purely position controller with state constraints is employed to verify the efficiency and effectiveness of the proposed motion adaptive method. We first set three cases with different desired contacting force whose control parameters are all chosen the same as Table. I. The robot starts from different random positions and then moves at a free space along with the desired DS. While contacting with surface of body, the DS will be adjusted in terms of the impressing force measured by force sensor such that the probe is able to scan the skin compliantly under specific desired tracking force. As shown in the sub-graph, the probe presses deeper while the desired tracking force is set larger. After completing the scanning motion, the probe will be converged to a unified point finally.

Under the constraint controller, the tracking error of adaptive DS motion can be restricted within a specific limitation which enable the controller not be disturbed by the interacting force as shown in Fig. 8. From the results, we can note that tracking errors are always close to zeros (less than ± 0.05) despite the robot is scanning along with the body.

In spite of verifying the compliant motion tracking performance of the proposed method, the force tracking experimental results are also shown in Fig. 9. In the experiments, the contacting force of normal vector is decomposed into two components, e.g. force in the horizontal X and vertical Z direction. In this case, we first set the desired force $F_d = 0$ in the process of free motion. Because of the zero wander of the force sensor, the measured contacting force will not be zero in spite of the free movement phase which may cause a negligible force tracking error.

VI. CONCLUSION

In this paper, a novel adaptive trajectory generating framework is proposed based on DS to tackle with the compliant interaction problem in the motion planning phase. Meanwhile, the proposed method is able to deal with dynamic force tracking problems incorporated the feedback of contacting force. In addition, passivity analysis based on iterative learning is adopted to update the potential factor in DS so as to satisfy the criterion of stability of adaptive DS during the interaction. Simulations are conducted to valid the effectiveness, stability and generalization of proposed methodology. Therefore, with the help of proposed adaptive DS, a compliant behavior can be achieve only by using position control which has brought a novel insight for robotic research. In the future, the proposed method will be considered the force constraint problems which is able to improve the safety of compliant interaction towards the unknown environment.

REFERENCES

- [1] W. Sheng, A. Thobbi, and Y. Gu, "An integrated framework for human-robot collaborative manipulation," *IEEE Transactions on Cybernetics*, vol. 45, no. 10, pp. 2030–2041, 2017.
- [2] X. Gao, J. Ling, X. Xiao, and M. Li, "Learning force-relevant skills from human demonstration," *Complexity*, vol. 2019, 2019.
- [3] S. Chen, F. Wang, Y. Lin, Q. Shi, and Y. Wang, "Ultrasound-guided needle insertion robotic system for percutaneous puncture," *International Journal of Computer Assisted Radiology and Surgery*, no. 4, 2021.
- [4] X. Fong, S. Natarajan, and M. O. Culjat, "Robotic ultrasound systems in medicine," *IEEE Transactions on Ultrasonics, Ferroelectrics, and Frequency Control*, vol. 60, no. 3, pp. 507–523, 2013.
- [5] R. Mebarki, A. Krupa, and F. Chaumette, "2-d ultrasound probe complete guidance by visual servoing using image moments," *IEEE Transactions on Robotics*, vol. 26, no. 2, pp. 296–306, 2010.
- [6] J. Solis, R. Nakadate, A. Takanishi, E. Minagawa, M. Sugawara, and K. Niki, "Out-of-plane visual servoing method for tracking the carotid artery with a robot-assisted ultrasound diagnostic system," in *IEEE International Conference on Robotics & Automation*, 2011.
- [7] A. Rykkje, J. F. Carlsen, and M. B. Nielsen, "Hand-held ultrasound devices compared with high-end ultrasound systems: A systematic review," *Diagnostics*, vol. 9, no. 2, 2019.
- [8] C. Delgorge, F. Courreges, L. A. Bassit, C. Rosenberger, N. Smith-Guerin, C. Bru, R. Gilabert, M. Vannoni, and G. Poisson, "A tele-operated mobile ultrasound scanner using a light-weight robot," *IEEE Transactions on Information Technology in Biomedicine*, vol. 9, no. 1, pp. 50–58, 2005.
- [9] X. Liu, S. S. Ge, F. Zhao, and X. Mei, "Optimized interaction control for robot manipulator interacting with flexible environment," *IEEE/ASME Transactions on Mechatronics*, vol. PP, no. 99, pp. 1–1, 2020.
- [10] M. Akbari, J. Carriere, T. Meyer, R. Sloboda, and M. Tavakoli, "Robotic ultrasound scanning with real-time image-based force adjustment: Quick response for enabling physical distancing during the covid-19 pandemic," *Frontiers in Robotics and AI*, vol. 8, p. 645424, 2021.
- [11] F. Conti, J. Park, and O. Khatib, "Interface design and control strategies for a robot assisted ultrasonic examination system," *Springer Tracts in Advanced Robotics*, vol. 79, pp. 97–113, 2014.
- [12] S. Onogi, Y. Urayama, S. Irisawa, and K. Masuda, "Robotic ultrasound probe handling auxiliary by active compliance control," *Advanced Robotics*.
- [13] A. Billard, S. Calinon, R. Dillmann, and S. Schaal, "Robot programming by demonstration," *Springer Berlin Heidelberg*, 2008.
- [14] Khansari-Zadeh, S. Mohammad, Billard, and Aude, "Learning stable nonlinear dynamical systems with gaussian mixture models." *IEEE Transactions on Robotics*, 2011.
- [15] A. J. Ijspeert, J. Nakanishi, H. Hoffmann, P. Pastor, and S. Schaal, "Dynamical movement primitives: Learning attractor models for motor behaviors," *Neural Computation*, vol. 25, no. 2, pp. 328–373, 2013.
- [16] A. Lemme, K. Neumann, R. F. Reinhart, and J. J. Steil, "Neural learning of vector fields for encoding stable dynamical systems," *Neurocomputing*, vol. 141, pp. 3–14, 2014.
- [17] T. Triquet, M. Khoramshahi, and A. Billard, "Task-adaptation for assistive robotics using switching dynamical systems," Tech. rep. LASA-EPFL, Tech. Rep., 2017.
- [18] Todorov, Emanuel, Jordan, and I. Michael, "Optimal feedback control as a theory of motor coordination." *Nature Neuroscience*, 2002.
- [19] H. Kambara, A. Takagi, H. Shimizu, T. Kawase, N. Yoshimura, N. Schweighofer, and Y. Koike, "Computational reproductions of external force field adaption without assuming desired trajectories," *Neural Networks*, vol. 139, pp. 179–198, 2021.
- [20] M. Khoramshahi, A. Laurens, T. Triquet, and A. Billard, "From human physical interaction to online motion adaptation using parameterized dynamical systems," in *2018 IEEE/RSJ International Conference on Intelligent Robots and Systems (IROS)*. IEEE, 2018, pp. 1361–1366.
- [21] W. Amanhoud, M. Khoramshahi, and A. Billard, "A dynamical system approach to motion and force generation in contact tasks," in *Robotics: Science and Systems 2019*, 2019.
- [22] W. Wei and C. Wen, "Adaptive actuator failure compensation control of uncertain nonlinear systems with guaranteed transient performance - sciencedirect," *Automatica*, vol. 46, no. 12, pp. 2082–2091, 2010.
- [23] Z. Ding, C. Xi, L. An, J. Dong, and Q. Zhang, "Prescribed performance switched adaptive dynamic surface control of switched nonlinear systems with average dwell time," *IEEE Transactions on Systems Man & Cybernetics Systems*, vol. 47, no. 7, pp. 1257–1269, 2017.
- [24] Y. J. Liu and S. Tong, "Barrier lyapunov functions-based adaptive control for a class of nonlinear pure-feedback systems with full state constraints," *Automatica*, vol. 64, no. C, pp. 70–75, 2016.
- [25] M. Saveriano and D. Lee, "Learning barrier functions for constrained motion planning with dynamical systems," in *IEEE/RSJ International Conference on Intelligent Robots and Systems*, 2019.
- [26] N. Hogan, "Impedance control : An approach to manipulator," *Journal of Dynamic Systems Measurement & Control*, vol. 107, 1985.
- [27] A. Kramberger, E. Shahriari, A. Gams, B. Nemec, and S. Haddadin, "Passivity based iterative learning of admittance-coupled dynamic movement primitives for interaction with changing environments," in *2018 IEEE/RSJ International Conference on Intelligent Robots and Systems (IROS)*, 2018.
- [28] H. Huang, C. Yang, and C. Chen, "Optimal robot-environment interaction under broad fuzzy neural adaptive control," *IEEE Transactions on Cybernetics*, vol. PP, no. 99, pp. 1–12, 2020.
- [29] S. M. Khansari-Zadeh and A. Billard, "Learning control lyapunov function to ensure stability of dynamical system-based robot reaching motions," *Robotics & Autonomous Systems*, vol. 62, no. 6, pp. 752–765, 2014.
- [30] H. Huang, C. Yang, and C. Y. Su, "Compliant motion adaptation with dynamical system during robot-environment interaction," 2020.
- [31] S. M. Khansari-Zadeh and A. Billard, "Imitation learning of globally stable non-linear point-to-point robot motions using nonlinear programming," in *2010 IEEE/RSJ International Conference on Intelligent Robots and Systems*. IEEE, 2010, pp. 2676–2683.



intelligent control.

Haohui Huang received the B.S. degree in automation from Guangdong University of Technology, Guangzhou, China, in 2011, and the M.S. degree in control science and engineering from Guangdong University of Technology, Guangzhou, China, in 2014 and Ph.D. degree in Control Science and Engineering from South China University of Technology, Guangzhou, China, in 2020. He is currently a postdoctoral in School of Electronic Information and Electrical Engineering, Shanghai Jiao Tong University. His research interests include robotics and



Yi Guo received his Ph.D. degree from Hong Kong University of Science and Technology in 2015 and B.S. degree from Shanghai Jiao Tong University in 2011. He is currently a research assistant professor in Department of Automation at Shanghai Jiao Tong University. His research interests include robot perception and autonomous control system design, Internet of Thing (IoT) and mobile computing.



tion planning and scheduling, discrete event dynamics systems, and computer integrated manufacturing.

Genke Yang received the B.S. degree in mathematics from Shanxi University, in 1984, the M.S. degree in mathematics from Xinan Normal University, in 1987, and the Ph.D. degree in systems engineering from Xian Jiaotong University, in 1998. He has been a full-time Professor with the Department of Automation, Shanghai Jiao Tong University, Shanghai, China. He is currently a member of the Collaborative Innovation Center for Advanced Ship and Deep-Sea Exploration, Shanghai. His research interests include supply chain management, logistics, production



Jian Chu received the B.S., M.S., and Ph.D. degrees from Zhejiang University, Hangzhou, China, in 1982, 1984, and 1989, respectively, and the Ph.D. degree in Joint Education Program from Zhejiang University and Kyoto University, Kyoto, Japan. He was a Post-Doctoral Researcher with the Institute of Advanced Process Control, Zhejiang University, where he was a Full Professor in 1993, and a Doctorial Advisor in 1994. He is now the chief researcher of Shanghai Jiao Tong University. His current research interests include control theory and

applications, research and development of computer control systems, and advanced process control software.



Xinwei Chen is with College of Computer and Control Engineering, Minjiang University, Fujian Provincial Key Laboratory of Information Processing and Intelligent Control, Fuzhou, 351008, China. He received his B.S., M.S. and Ph.D both in Computer Science and Intelligent Robot System from Nankai University, in 2006, 2009 and 2012. His current research interests include Intelligent Robot System, Embeded System and Computer Vision. His current projects cover the topics from mobile robot, 3D Printing Robot, inhabitable island obser-

vation system and so on.



Zhibin (Alex) Li is an Associate Professor at the Department of Computer Science, University College of London. He obtained a joint PhD degree in Robotics at the Italian Institute of Technology (IIT) and the University of Genova in 2012. His research interests are in creating intelligent robots and machines with human comparable abilities to locomote and manipulate, and inventing new hardware and software for control, optimization, and deep learning of robot motor skills.



Chenguang Yang (M'10-SM'16) received the Ph.D. degree in control engineering from the National University of Singapore, Singapore, in 2010, and postdoctoral training in human robotics from the Imperial College London, London, U.K. He was awarded UK EPSRC UKRI Innovation Fellowship and individual EU Marie Curie International Incoming Fellowship. As the lead author, he won the IEEE Transactions on Robotics Best Paper Award (2012) and IEEE Transactions on Neural Networks and Learning Systems Outstanding Paper Award (2022).

He is a Co-Chair of IEEE Technical Committee on Collaborative Automation for Flexible Manufacturing (CAFEM) and a Co-Chair of IEEE Technical Committee on Bio-mechatronics and Bio-robotics Systems (B2S). He serves as Associate Editors of a number of international top journals including seven IEEE Transactions. His research interest lies in human robot interaction and intelligent system design.